Journal of Hydrology 519 (2014) 670–682

Contents lists available at ScienceDirect

Journal of Hydrology

journal homepage: www.elsevier.com/locate/jhydrol

Regionalization of subsurface stormflow parameters of hydrologic models: Derivation from regional analysis of streamflow recession curves

Sheng Ye [a], Hong-Yi Li [b], Maoyi Huang [b], Melkamu Ali [c], Guoyong Leng [b], L. Ruby Leung [b], Shao-wen Wang [a], Murugesu Sivapalan [a,d,*]

[a] Department of Geography and Geographic Information Science, University of Illinois at Urbana-Champaign, Urbana, IL, USA
[b] Pacific Northwest National Laboratory, 902 Battelle Boulevard, Richland, WA 99352, USA
[c] Dipartimento di Scienze dell'Ingegneria Civile, Universita di Roma Tre, Via Vito Volterra 62, 00146 Rome, Italy
[d] Department of Civil and Environmental Engineering, University of Illinois at Urbana-Champaign, Urbana, IL, USA

ARTICLE INFO

Article history:
Received 1 October 2013
Received in revised form 23 June 2014
Accepted 12 July 2014
Available online 21 July 2014
This manuscript was handled by Konstantine P. Georgakakos, Editor-in-Chief, with the assistance of Yu Zhang, Associate Editor

Keywords:
Subsurface flow
Closure relations
Storage–discharge relationship
Recession–slope curve
Statistical methods

SUMMARY

Subsurface stormflow is an important component of the rainfall–runoff response, especially in steep terrain. Its contribution to total runoff is, however, poorly represented in the current generation of land surface models. The lack of physical basis of these common parameterizations precludes *a priori* estimation of the stormflow (i.e. without calibration), which is a major drawback for prediction in ungauged basins, or for use in global land surface models. This paper is aimed at deriving regionalized parameterizations of the storage–discharge relationship relating to subsurface stormflow from a top–down empirical data analysis of streamflow recession curves extracted from 50 eastern United States catchments. Detailed regression analyses were performed between parameters of the empirical storage–discharge relationships and the controlling climate, soil and topographic characteristics. The regression analyses performed on empirical recession curves at catchment scale indicated that the coefficient of the power-law form storage–discharge relationship is closely related to the catchment hydrologic characteristics, which is consistent with the hydraulic theory derived mainly at the hillslope scale. As for the exponent, besides the role of field scale soil hydraulic properties as suggested by hydraulic theory, it is found to be more strongly affected by climate (aridity) at the catchment scale. At a fundamental level these results point to the need for more detailed exploration of the co-dependence of soil, vegetation and topography with climate.

© 2014 Elsevier B.V. All rights reserved.

1. Introduction

Land surface processes are an integral part of the Earth system. By regulating surface moisture and heat fluxes, land surface processes can provide important feedbacks to climate and influence the regional and global hydrologic cycle (e.g., Koster et al., 2004; Seneviratne et al., 2010). To improve predictions of future climate, it is crucial to understand and constrain uncertainty stemming from parameterizations used in land surface models (LSMs). Recently Hou et al. (2012) and Huang et al. (2013) used an uncertainty quantification framework to assess hydrologic parameter uncertainties in Version 4 of the Community Land Model (CLM4) (Lawrence et al., 2011). Applying their framework to 13 flux towers and 20 catchments across the US spanning a wide range of climate and landscape characteristics, they found that the simulated land surface water and energy fluxes as well as runoff showed the largest sensitivity to parameters related to subsurface runoff generation (Niu et al., 2005, 2007). This highlights the need to improve subsurface runoff generation schemes in LSMs at the hillslope scale.

As shown by several previous studies, subsurface runoff generation can be parameterized using storage–discharge relationships of a power law form, which can capture the asymmetric response of subsurface hydrologic processes to floods and droughts (e.g., Eltahir and Yeh, 1999; Liang et al., 2003). Such parameterizations, including the TOPMODEL approach (Beven and Kirkby, 1979; Beven et al., 1984; Beven, 1997) included in CLM4 and the ARNO model (Francini and Pacciani, 1991; Todini, 1996), are now widely

* Corresponding author at: Department of Geography and Geographic Information Science, University of Illinois at Urbana-Champaign, Urbana, IL, USA.
E-mail address: sivapala@illinois.edu (M. Sivapalan).

http://dx.doi.org/10.1016/j.jhydrol.2014.07.017
0022-1694/© 2014 Elsevier B.V. All rights reserved.

used in LSMs (e.g., Liang et al., 1994; Huang and Liang, 2006; Warrach et al., 2002; Niu et al., 2005, 2007; Oleson et al., 2010, 2013; Ringeval et al., 2012), although each approach still suffers from limitations and can be further improved. Recent reviews on the advantages and disadvantages of these parameterizations can be found in Huang and Liang (2006), Huang et al. (2008), and Li et al. (2011). A particular challenge in applying these parameterizations in Earth system models is the limited availability of naturalized streamflow data for calibrating model parameters globally, and reducing the dependence of parameterizations on calibrations is a key requirement. This is the first of a two-part paper (the other being Ali et al., 2014) that aims towards developing improved parameterizations of shallow subsurface flow for land surface models such as CLM4, expressed in terms of the power-law form of a lumped storage–discharge relationship:

$$Q = aS^b \tag{1}$$

where Q is subsurface flow and S is saturated subsurface storage. To be consistent with recession curves observed at the catchment outlet, Q and S are also defined at the catchment scale with Q as the aggregated subsurface flow and S as the average storage for the whole catchment. As a result, a and b are parameters that represent the aggregated effects of land surface heterogeneity (i.e., of both soil hydraulic properties and topography) at the catchment scale. Ideally, for subsurface flow to be predicted using Eq. (1) without calibration (e.g., in ungauged basins or landscapes), the parameters a and b must be estimated *a priori* on the basis of measurable landscape characteristics. Such a parameterization of the subsurface flow must capture the effects of soil and landscape properties in a simple way, accounting for the effects of spatial heterogeneity without the need to resolve flows at smaller scales explicitly. This is the motivation for the work behind this paper. We have approached this estimation problem from two alternative perspectives: (i) empirical (top–down), and (ii) theoretical (bottom–up).

The theoretical (or bottom–up) approach (see accompanying paper by Ali et al., 2014) involves the use of numerical simulations that help to derive closure relations through application of detailed, distributed physically based hydrological models using appropriate boundary conditions and assumed forms of spatial variability of soil and topographic properties (Robinson and Sivapalan, 1995; Viney and Sivapalan, 2004). We categorize the spatial heterogeneities entering the problem here as (i) within hillslope, where the heterogeneity is assumed to relate to soil only, and topography is taken to be constant, and (ii) between hillslopes, where the heterogeneity arising from topography is explicitly resolved, while the effects of within-hillslope heterogeneity of soil properties is parameterized from (i). The theoretical approach of Ali et al. (2014) is based on Richards equation based simulations at the hillslope scale, parameterizing the effects of within-hillslope heterogeneity and their subsequent up-scaling to the catchment scale, incorporating the effects of topographic variability between hillslopes.

The empirical (or top–down) approach (the subject of this paper) involves (i) making inferences of the storage–discharge relationships, and associated parameters a and b, directly at the catchment scale on the basis of analysis of observed streamflow recession curves in a large number of catchments, followed by (ii) multiple regression analyses of the estimated recession parameters a and b against measurable climatic and landscape (soils and topography) characteristics.

The streamflow recession curve (Brutsaert and Nieber, 1977) is one of the most widely used catchment runoff signatures, and provides insights into the subsurface flow generation processes (Tague and Grant, 2004). By measuring how river flow recedes at the end of a storm event, it can reveal the internal hydrologic dynamics at catchment scale as a holistic measure of the catchment's drainage characteristics (Troch et al., 2013). Many studies have been conducted to interpret the recession flow based on hydraulic groundwater theory, such as the Boussinesq equation (Troch et al., 2013). For convenience, the recession behavior of the catchment is often expressed in terms of the so-called recession–slope curve, the relationship between the rate of decline rate of flow ($-dQ/dt$) and Q:

$$-\frac{dQ}{dt} = \alpha Q^{\beta} \tag{2}$$

Note that the parameters α and exponent β may vary with time during the year due to the effect of seasonality of evaporation loss (Wittenberg and Sivapalan, 1999; Shaw and Riha, 2012), which can be minimized by focusing on periods when evaporation is minimal (e.g., winter) or by explicitly accounting for the evaporation loss. Provided this is done, it can then be deemed a unique signature of the catchment response. The coefficient α and exponent β can be directly estimated from observed recession curves by curve fitting, and reflect the net effects of the population of hillslopes (of various sizes and shapes) and the soils that constitute the catchment.

Considerable work has been carried out to derive analytical solutions to the Boussinesq equation governing saturated subsurface drainage from an unconfined homogeneous aquifer into the river below to aid the deciphering of the physical meaning and controls of both recession parameters α and β. Several studies have explored the effects of catchment-scale heterogeneity on the shape of the recession curves. These theoretical studies suggest that the shapes of the recession curves are strongly affected by soil hydraulic conductivity and its vertical and horizontal (downslope) heterogeneity (Rupp and Selker, 2005, 2006a,b; Troch et al., 2008; Harman et al., 2009). Landscape geomorphologic features too can contribute to the shape of the recession curves (Biswal and Marani, 2010; Harman et al., 2009; Lyon and Troch, 2010). However, due to the many simplifying assumptions and lack of data, most of the pioneering studies in this area have been largely theoretical, and only a few went further and validated the equations derived on the basis of the recession curves in real catchments (Harman et al., 2009; Lyon and Troch, 2010).

The storage–discharge relationship that we are interested in can be derived from the recession–slope curve in a straightforward manner by utilizing the relationship that exists between parameters a and b of the storage–discharge relationship and the parameters α and β of the recession–slope curve. From Eqs. (1) and (2), we obtain the derivative of storage (S):

$$\frac{dS}{dt} = \frac{d}{dt}\left\{\left(\frac{Q}{a}\right)^{1/b}\right\} = \frac{Q^{1/b-1}}{ba^{1/b}}\frac{dQ}{dt} = -\frac{\alpha}{ba^{1/b}}Q^{1/b-1+\beta} \tag{3}$$

When the impact of evaporation is negligible, $dS/dt = -Q$, and combining this with Eq. (3) yields:

$$a = [\alpha(2-\beta)]^{1/(2-\beta)} \tag{4a}$$

$$b = \frac{1}{2-\beta} \tag{4b}$$

In this study, we explore the nature of the storage–discharge relationship and its controls through empirical analysis of the recession curve data from hundreds of catchments across the continental United States, and their connection to measureable catchment characteristics such as topography, soil properties, and other geomorphologic features.

The theoretical (or bottom–up) approach will follow in the second paper of the series (Ali et al., 2014), which can yield results that are physically consistent, but their applicability in actual catchments is hampered by our inability to fully characterize the

heterogeneity of soils (and even some aspects of topography) present in actual catchments, including especially the self-organized heterogeneity that is often present, such as soil catena, and the presence of macro-pores and other preferred pathways, whose effects on flow are difficult to characterize in terms of the Richards equation. On the other hand, empirical relationships extracted from observed recession curves, such as those presented in this paper, are much more realistic in terms of what may emerge at the catchment scale, but are empirical rather than physics-based, which makes them difficult to interpret physically and to extrapolate from gauged to ungauged basins. Success in our quest for physically based closure relations for subsurface flow will come only through a reconciliation of the outcomes of both the empirical (top–down) and theoretical (bottom–up) approaches. This will be pursued in subsequent research, and may be the subject of a future publication.

This paper, which presents the outcomes of the empirical (top–down) approach, begins with a summary of the data (climate and streamflow data, and detailed information on catchment characteristics) presented in Section 2 that also describes the methodology that is used to extract the coefficient and exponent from the recession curves. Section 3 presents the spatial (regional) distribution of the parameters α and β across the continental US, and their interpretation. This is followed, in Section 4, by a variable selection scheme that is used to define the most important climate and catchment characteristics that determine the observed recession behaviors, along with the validation of the so-derived empirical relationships. Section 5 summarizes the main outcomes of the study, their connection to the results of the modeling work (Ali et al., 2014), and possible avenues towards synthesis.

2. Data and methodology

2.1. Data

This study is carried out with the climate and flow data and topographic information taken from the Model Parameter Estimation Experiment (MOPEX) dataset, drainage density data extracted from the National Hydrography Dataset (NHD) (http://nhd.usgs.gov/), and soil properties from the USGS SSURGO dataset (http://soils.usda.gov/survey/geography/ssurgo/). The MOPEX dataset (http://www.nws.noaa.gov/oh/mopex/index.html) provides daily climate and streamflow data from 438 catchments across the continental US, covering a wide range of climate conditions, landscapes, and ecosystems, ranging from very humid environments on the north-west coast to extremely arid conditions in New Mexico. Using aridity index (*AI*, the ratio of mean annual potential evaporation to mean annual precipitation) to quantify the climate, the *AI* of these 438 catchments ranges from 0.25 (humid) to 5.5 (very arid). The MOPEX dataset includes catchments of different drainage areas, ranging from 66 km^2 to 10,328 km^2, consisting of very flat (<1%) to very steep (10%) hillslopes, permitting the derivation of recession curves for a wide range of catchment conditions. Of the 438 catchments, 428 catchments with longer than 10 years of continuous historical data are used in this study to estimate the recession curve parameters α and β.

Subsequently, a subset of 50 of these MOPEX catchments are selected to generate regional relationships between the recession curve parameters and several measureable climatic and landscape characteristics. Fig. 1 depicts the 50 selected catchments, which are devoid of such obvious data problems. General information on the selected catchments is provided in Table 1.

These catchments were chosen under the following criteria to minimize the influence from other confounding factors. (1) Reasonable number of flow events to minimize the effects of data insufficiency on the recession curve parameters (i.e., at least two events per year on average for more than 30 years). The extreme arid catchments in the south-west were avoided (e.g., Arizona, Texas) as there are only a few flow events (usually less than ten) during the entire record period, and some of the events are too small to perform recession analysis. The recession parameters extracted from such a small number of events could be biased and may not be representative. (2) Minimal impact of regional groundwater and/or snowmelt. Mountainous catchments with significant snowmelt influence (i.e., ID, WY, etc.) were excluded due to the overwhelming dominance of snowmelt detected in the previous modeling study (Ye et al., 2012): these catchments tend to have just one single large event that occurs each year in late spring or early summer caused by snowmelt, with almost no events occurring in winter (Ye et al., 2012). Since our goal is to understand the natural storage–discharge relationship from the recession curve analysis, in order to focus on this and minimize the impact of other factors, we removed these catchments from further consideration. (3) Minimal human impact. Although most MOPEX catchments have limited human influence, considerable human activities such as agriculture are still present in several Mid-western catchments (Wang and Hejazi, 2011). In the presence of artificial water extraction (Hatfield et al., 2009) and tile drainage (Li et al., 2010), the recession parameters derived from data are not representative of the natural storage–discharge relationships. Hence these Midwestern catchments identified in the previous modeling work (Ye et al., 2012) were not taken into account either. (4) Complete data coverage. Since the soil dataset we used (i.e., SSURGO) has not been extended to fully cover the western states (i.e., WA, CA) when this study was conducted, we focused on the catchments with complete soil data coverage.

From the remaining catchments that met these criteria, which are mainly located in the eastern part of the continental US, we then selected 50 catchments exhibiting broad ranges of variation of drainage area, climate, and landscape properties. The number of 50 was decided due to two considerations: (1) to keep the efforts of SSURGO data processing (conducted for each individual catchment) to a reasonable level and (2) to have a sufficiently large sample of catchments. A rigid variable selection algorithm (discussed in detail in Section 2.2.2) is applied to minimize the potential biases in this sample set. Even though these catchments were located in the more humid part of the United States, they still represent a significant range (0.3–1.5) of the aridity index. Further work is needed to validate the findings of this study in more arid regions, or those dominated by factors other than the natural storage–discharge relationship, such as snowmelt or land use changes.

Candidate predictors are chosen based on the knowledge from the literature including both the hydraulic theory and the heterogeneity hypothesis (Brutsaert and Lopez, 1998; Rupp and Selker, 2006a,b; Harman et al., 2009) as well as the parameters required in the companion modeling work (Ali et al., 2014). We also assembled other predictors that may have an impact on stormflow generation but are not usually considered in analytical studies based on groundwater theory (i.e. aridity index). Consequently, the aridity index (*AI*), topographic slope (θ), the mean (K_s) and standard deviation (σ_{Ks}) of saturated hydraulic conductivity at the surface, the vertical (exponential) decay parameter of the saturated hydraulic conductivity (f), soil porosity (ϕ), soil depth (d) and drainage density (D_d) were estimated for the selected catchments. As the two parameters used to estimate the topographic wetness index are already included (slope and catchment area factored in the drainage density), we chose not to include it here in order to reduce repetition and the correlation between predictors. The drainage density was estimated from the NHD dataset as the ratio of the total channel length within a catchment to the catchment area. Although the MOPEX dataset also provides estimates of

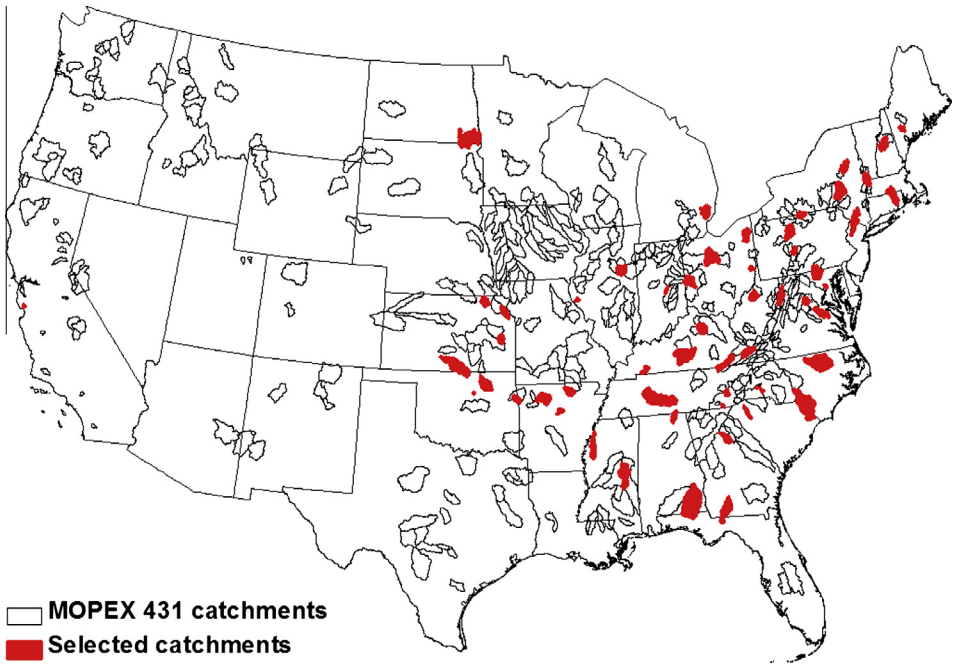

Fig. 1. Map of the selected catchments.

Table 1
Characteristics of the 50 selected catchments.

	Min	Mean	Max
α	0.02	0.10	0.25
β	0.99	1.46	1.91
Area (km^2)	66.60	1731.02	9062.40
Aridity index	0.39	0.82	1.5
Slope (degree)	0.41	5.72	22.84
Mean saturated hydraulic conductivity at surface (μm/s)	2.5	18.70	74.60
Standard deviation of saturated hydraulic conductivity at surface	1.27	12.13	31.88
Drainage density (km/km^2)	0.04	0.62	1.91
Depth × porosity (m)	0.18	0.48	0.70
Vertical decay parameter of the saturated hydraulic conductivity (m^{-1})	0.11	0.81	2.36

saturated hydraulic conductivity, it was an earlier qualitative estimate based on soil texture, and the resolution was deemed too coarse for this study. Therefore, we used the USGS SSURGO dataset (http://soildatamart.nrcs.usda.gov) to extract the mean and standard deviation of the saturated hydraulic conductivity at the surface and also a vertical exponential decay parameter. The SSURGO dataset is provided by the National Resource Conservation Service (NRCS); it includes both spatial data of the measured map unit, and tabular data of the measurements done within each map unit. Although the coverage of the SSURGO dataset is not as wide as the earlier version of the USGS State Soil Geographic (STATSGO) soils data, we chose to use the SSURGO dataset for this study due to its higher resolution and better data quality. The STATSGO dataset was generated for multi-state, regional, and state level analysis, with the map scale compiled at a scale of 1:250,000, while the SSURGO dataset is compiled at the scales of 1:12,000 and 1:24,000. That is, the resolution of the SSURGO dataset is about 10 times higher than the STASGO dataset (Earls and Dixon, 2005; Bliss et al., 2010). The quality of soil databases is also higher in the SSURGO dataset as the result of the NRCS efforts (Bliss et al., 2010) to provide more precise and detailed spatial and vertical measurements (Anderson et al., 2006). As we will learn from the results, the soil hydraulic properties play a critical role in the subsurface flow generation process, and the SSURGO dataset fits our interest better despite of the more limited coverage.

2.2. Methodology

2.2.1. Data processing

The recession periods in the continuous multi-year hydrographs were extracted by an automatic algorithm developed by Vogel and Kroll (1992) whose study catchments were similar in climate to ours. Based on the 3-day moving average of a hydrograph, the falling limb is defined as the segment between each pair of peaks and valleys. To avoid the influence of overland flow, only the late 70% of a falling limb was recorded as a recession period. To remove possible noise from small events and large fluctuations during big events, only recession periods longer than 10 days were selected, and also recessions with peak flows less than the 10th percentile were excluded.

Instead of the criteria used by Brutsaert and Nieber's (1977), who defined recessions as flow periods when the rainfall ends, we adopted Vogel and Kroll's (1992) algorithm for the recession period selection since it helps to retain a considerable amount of records for analysis and individual events without discontinuity in the records. Many of our catchments are located along the east coast of the United States (e.g., NY, VA, MA, etc.) where rainfall happens all year round. Given the relatively coarse temporal resolution (daily time scale), it is hard to retrieve recession curves long enough without interruption by subsequent rainfall events to give meaningful regression results. Although we will fit the regression

model to all the qualified recessions, because of the potential variation with time due to changes in evaporation and other confounding factors (Shaw and Riha, 2012), we would like to retain each individual event as completely as possible. Comparing with Brutsaert and Nieber's (1977) algorithm, Vogel and Kroll's (1992) selection procedure keeps nearly twice the data records (about 13% of the total time period according to Stoelzle et al., 2013). As Stoelzle et al. (2013) pointed that a larger number of data points could help reduce the sensitivity in the fitting and is more influential on parameterization than the choice of parameterization method. Due to the limited amount of events during the winter period we are looking at, Vogel and Kroll's (1992) selection procedure is chosen to keep as many qualified recession records as possible. The moving average processing also helps to reduce the horizontal scatter in the recession plots created by low dQ/dt values, which can have considerable impact on the recession parameter calculation (Stoelzle et al., 2013). Fig. 2 shows an example of recession periods identified using our criteria.

Taking the natural logarithm of Eq. (2), we then have the linear relationship:

$$\ln\left(-\frac{dQ}{dt}\right) = \ln\alpha + \beta\ln Q \tag{5}$$

This relationship is used to fit the extracted recession curve data as:

$$\ln(Q_{t-1} - Q_t) = \ln\alpha + \beta\ln\left(\frac{Q_t + Q_{t+1}}{2}\right) \tag{6}$$

where t is the tth day of a recession record, Q_{t-1}, Q_t, Q_{t+1} are the flow over three consecutive days. The nature of the flow data available in the MOPEX catchments dictated the choice of a day as the time increment. A regular linear regression fitting model is used to calculate α and β in this study instead of the lower envelope method in order to minimize the bias that may be caused by the data quality. The transition range between the upper part (the early stage of recession) and lower part (the late stage) is wide (Szilagyi et al., 1998), and hence it is hard to define the lower part from data alone. The lower envelope method is not only sensitive to the quality of streamflow data and could also be biased by the recession periods extracted (Stoelzle et al., 2013). Given the temporal resolution of MOPEX data set, to avoid the potential bias in the fitting due to the data quality, we adopted the regular linear regression fitting model in order to get a relatively stable result. Initial evaluation of α and β values at the monthly scale showed significant seasonal variation in several regions: the monthly β tends to be steady and less variant in winter and early spring, and starts to rise in late spring, drops after early fall. A similar trend was also found in the analysis of individual recessions by Shaw and Riha (2012). This is due to the drying effects of evaporation (ET). As a way to minimize the influence of the unknown ET and to focus on the true natural storage–discharge relationship, in this study we used the α and β values extracted from recessions occurring during winter (December, January and February) only, when ET is deemed the lowest. Since winter is the relatively dry season in our study sites, this also helps to prevent the impact of channel-floodplain processes that occur during big flow events. Other factors such as snowmelt and low permeability due to frozen soil may cast an influence on winter events in the northern catchments, However, previous model development (Ye et al., 2012) has suggested that the snowmelt impact in our remaining study catchments are not dominant. This is also confirmed by the fact that we did not see significant differences between the trends of monthly β in the northern catchments (i.e. MA, NY) and southern catchments (i.e. GA, FL).

The aridity index (= PET/P based on mean annual estimates) was calculated from annual precipitation (P) and annual potential evapotranspiration (PET) data from the MOPEX dataset. The same was done for average topographic slope and soil porosity, which are provided in the MOPEX dataset. Drainage density (= L/A) was estimated from the stream length (L) and drainage area (A) extracted from NHD dataset.

The SSURGO data was downloaded as feature dataset by county. For this study, we needed the soil data at the catchment scale in a raster format so as to calculate the standard deviation. A procedure was developed to merge the SSURGO data, clip the data by the catchment boundary, retrieve the soil porosity (ϕ), which can be used to describe the soil water storage capacity when combined with soil depth (ϕd, saturated hydraulic conductivity at the top and bottom layer as well as the vertically averaged value for each map unit, and then convert the data to raster data type. These reconstructed raster data with the average porosity or saturated hydraulic conductivity at the surface were then used to compute the spatial average hydraulic conductivity value and its standard deviation.

We assumed that the saturated hydraulic conductivity decreases exponentially with depth:

$$K_b = K_s\exp(-fd) \tag{7}$$

where K_s, K_b are the surface and bottom saturated hydraulic conductivity, f is the decay parameter, and d is the soil depth. By integrating vertically from a depth of 0 to the total soil depth (d), the vertically averaged saturated hydraulic conductivity, K, can be calculated as:

$$K = \frac{1}{d}\int_0^d K_s\exp(-fd) = \frac{1}{fd}(K_s - K_s\exp(-fd)) \tag{8}$$

Substituting Eq. (7) into Eq. (8), we then obtain:

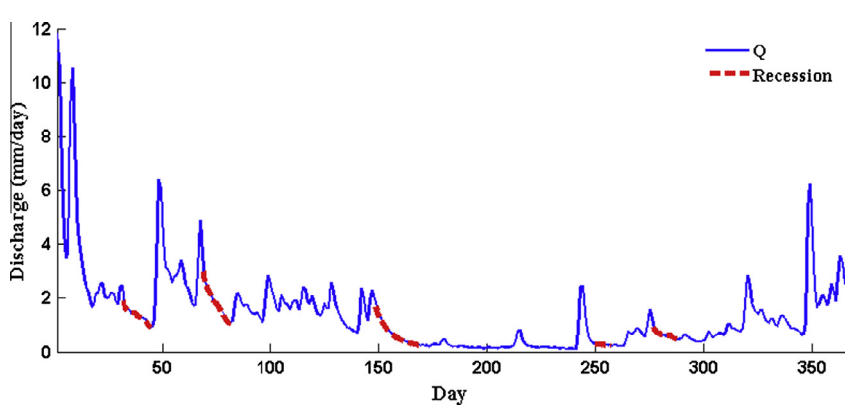

Fig. 2. Automatic separation of the recession periods. α and β are estimated for the recessions that occur during winter when the ET impact is smallest.

$$f = \frac{K_s - K_d}{Kd} \tag{9}$$

As the number of vertical measurements of saturated hydraulic conductivity at each sample column is small, there would be much uncertainty in the local estimation of the decay parameter. Each of these parameters is also highly variable in space, including the exponential decay parameter, *f*. In order to obtain a more robust estimate of *f* at the catchment scale and minimize the uncertainty, we estimated spatial (arithmetic) averages of both surface and bottom saturated hydraulic conductivity values using available point values, as well as the spatial average of their vertical mean, and a spatially average depth. Then it can be shown that the vertical decay parameter can be obtained from:

$$f = \frac{\overline{K}_s - \overline{K}_d}{\overline{K}\,\overline{d}} \tag{10}$$

where $\overline{K}_s$ is the spatially averaged surface saturated hydraulic conductivity, $\overline{K}_d$ is the spatially averaged bottom saturated hydraulic conductivity, $\overline{K}$ is the spatial average of the vertical mean saturated hydraulic conductivity, $\overline{d}$ is the spatial average of the surveyed soil depth. Clearly, this is only an approximate estimate of the exponential decay parameter, yet this is the best that can be achieved at such large scale, given the paucity of datasets currently available.

2.2.2. Parameter regionalization: variable selection procedure

Several recent studies have attempted to understand how soil properties and topographic and geomorphologic characteristics control subsurface flow generation in a quantitative way (Rupp and Selker, 2006a,b; Troch et al., 2008; Biswal and Marani, 2010). Estimated values of α and β in their original or logarithmic forms were first plotted against all the candidate predictors to derive individual relationships between the predictors and α and β. Although not all the relationships for the recession coefficient and exponent would be statistically significant, they provide information for down-selecting the predictors. In this paper, to determine the most influential factors, we experimented with different forms of the predictor and the response using linear regressions. Both α and β obtained from winter recessions and their natural logarithmic forms were used as the response in the linear regression, while all parameters including *AI*, slope, drainage density, porosity, soil depth, mean, standard deviation and vertical decay parameter of saturated hydraulic conductivity, and others, and their natural logarithmic forms were used as candidate predictors. A variable selection scheme was developed to eliminate redundant or insignificant predictors.

Due to the limited sample size, cross validation was employed to improve the reliability of the final selected regression model. That is, 75% of the data were randomly selected as training data used to fit the model and for the variable selection. After the selection, the remaining 25% of the data were used to validate the model selection results (Fig. 3). This cross-validation was conducted 50 times on average in order to reduce the potential bias in the sample selection (we repeated this three times and obtained similar results). The predictors retained by the model selection criteria and the R^2 of the validation in the test data were recorded each time. Finally, an averaged R^2 over all 50 validation tests is calculated and the frequency for each predictor chosen by the different criteria was also recorded. The predictors that were retained most often in all three methods were considered the most influential factors in predicting α and β derived from the recession curves.

Three statistical criteria were used in the variable selection: the Akaike Information Criterion (AIC), the Bayesian Information Criterion (BIC), and the *least absolute shrinkage and selection operator* (LASSO). The AIC is a statistical metric used in model selection, with a penalty term for increase in model size ($2k$), to choose the most suitable model with the least information loss (Akaike, 1974). It has also been applied to assess the necessary model complexity to get the required quality of model predictions (Engelhardt et al., 2012). For linear regression models, it can be computed as follows:

$$\mathrm{AIC} = -2\ln(\mathrm{Likelihood}) + 2k = n\ln\frac{\sum(\hat{y}-\bar{y})^2}{n} + 2k \tag{11}$$

where n is the sample size (= 50 here) and k is the number of predictors used in each model, $\hat{y}$ is the value of the response (i.e. α or β or their logarithmic forms) predicted by the fitted linear regression model, while $\bar{y}$ is the mean of the sample response. BIC is also a model selection criterion based on the likelihood function (Schwarz, 1978). Like AIC, it also has a penalty term for the increase in model size, but is larger than AIC ($k\ln(n)$):

$$\mathrm{BIC} = -2\ln(\mathrm{Likelihood}) + k\ln(n) = n\ln\frac{\sum(\hat{y}-\bar{y})^2}{n} + k\ln(n) \tag{12}$$

Both AIC and BIC select a subset of the candidate predictors. The variables are either retained or removed. This is a discrete process, which often leads to high variances and does not help reduce the error in the full model. The class of methods called shrinkage methods are more continuous and could avoid the high variability in AIC and BIC by estimating the regression coefficients that minimize the penalized residual sum of squares. LASSO is one of the shrinkage methods that do both shrinkage and variable selection by selecting those variables that minimize the following objective function (Hastie et al., 2009):

$$Z = ||y - \hat{y}||^2 + \lambda\sum|\omega_j| \tag{13}$$

where $\hat{y}$ is the value of the response (i.e. α, β or their logarithmic forms) predicted by the fitted linear regression model, y is the observed value of the sample response, λ is the coefficient to be optimized, ω_j is the coefficient of each of the predictors. A large λ will force some of the coefficients to be zero, which is part of the variable selection process. As a result, AIC is more focused on minimizing the prediction error, which favors larger models. BIC, in contrast, tends to select smaller models as it imposes larger penalty on the model size, while LASSO helps minimize the variance and is more consistent in selecting the models (Hastie et al., 2009). In this study, we tested all three methods, counted the times different predictors were selected by each method in the 50 tests, calculated the frequency they were selected by different methods, and lastly finalized a set of predictors that were more often retained than removed (that is, the frequency each predictor was chosen must be larger than 50%) in all three methods.

3. Results

3.1. The spatial patterns of α, β

Before we take a closer look at the 50 selected catchments, we look at the regional patterns of the regressed α, β values from the recession curves of all 428 catchments estimated from winter recessions to see if we can gain any insight into what could explain these patterns. These are presented in Fig. 4. Finding common catchment characteristics with similar ranges of α, β may provide clues about factors that may be relevant.

As we can see from the figure, α is generally smaller along the eastern and western coasts as well as the upper Midwest where climate is more humid, larger in catchments in or near the Appalachian Mountain, and is even larger in the semi-arid and high mountain regions of the west (NM, ID, AZ, etc.). There are some exceptions, e.g., in Texas, where some arid catchments also have small α values: this could be related to uncertainties in the model

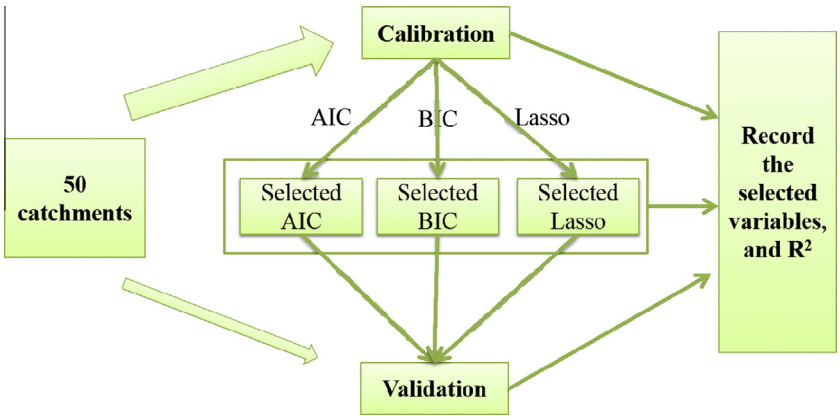

Fig. 3. Flow chart of the variable selection process.

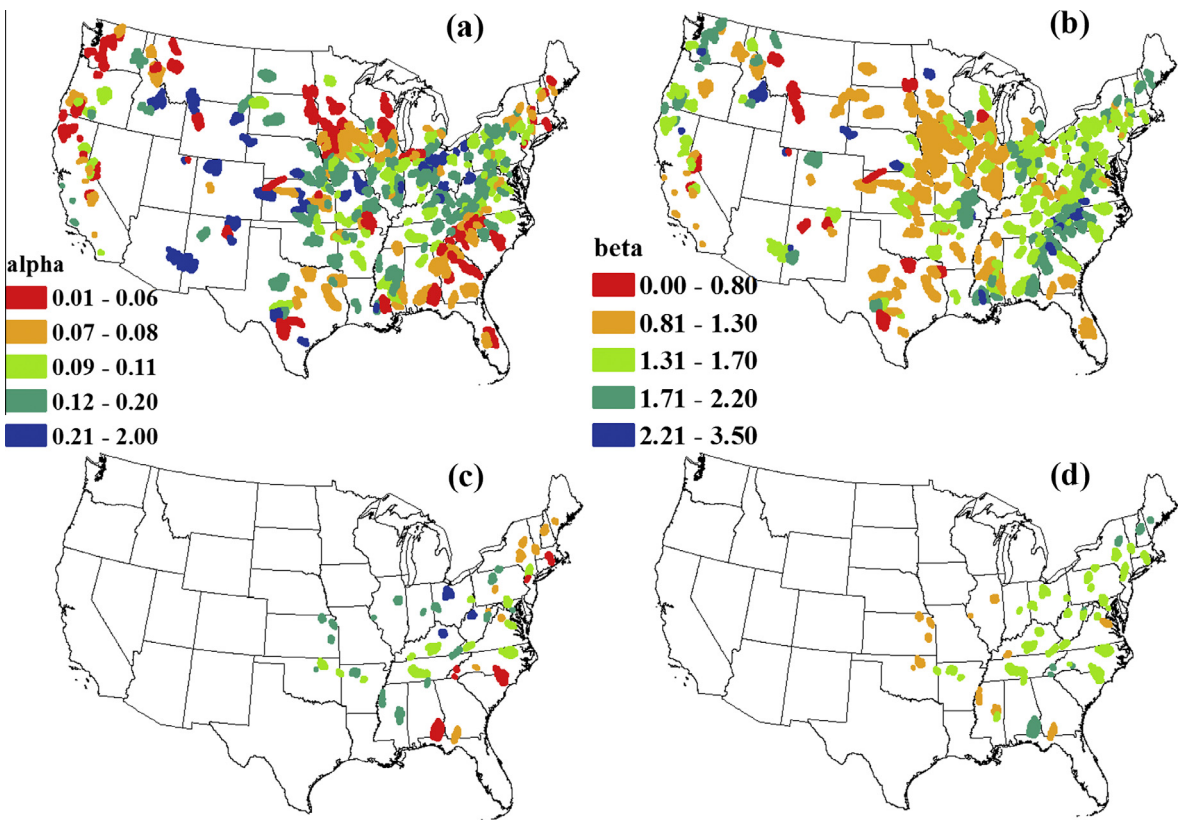

Fig. 4. Spatial distribution of (a) α for all the study sites; (b) β for all the study sites; (c) α for the selected sites; (d) β for the selected sites.

fitting and selection processes due to the ephemeral streams that limit the number of observations available from the 10 years record used for deriving the recession periods.

Fig. 4b illustrates the regional pattern of β, which exhibits a more diverse pattern. Roughly there is a decreasing trend in β from the coastal regions towards the interior. Specifically, β is around 2 in the catchments along the east coast except for those in Florida, it drops to values less than 1.5 in catchments in the central US. In the mid-western and western mountainous catchments, as well as in catchments in the arid southern US, β is around 1. Its value again increases to over 1.5 in catchments along the west coast. Looking at this in another way, β is large in humid and steep catchments near the Appalachian Mountain as well as along the western coastal range, but is small in extremely arid catchments in the south (i.e. NM, AZ, TX, etc.) and topographically flat catchments in the Midwest. An exception is that β is small in the coastal mountainous catchments in the West, which are humid as well as steep. This could be caused by the limited number of recessions studied here. As those catchments are dominated by a single flow event per year, from late spring to early summer, driven heavily by snowmelt. The significant snowmelt overwhelms the contribution from subsurface flow, leaving almost no flow events during winter, which leads to unreliable estimates of α and β.

3.2. Variable selection results

Fig. 5 presents the initial scatter plots of possible relationships between α and β and various climatic, geomorphologic and soil hydraulic properties for the 50 selected catchments: aridity index (AI), the drainage area, topographic slope (θ), drainage density

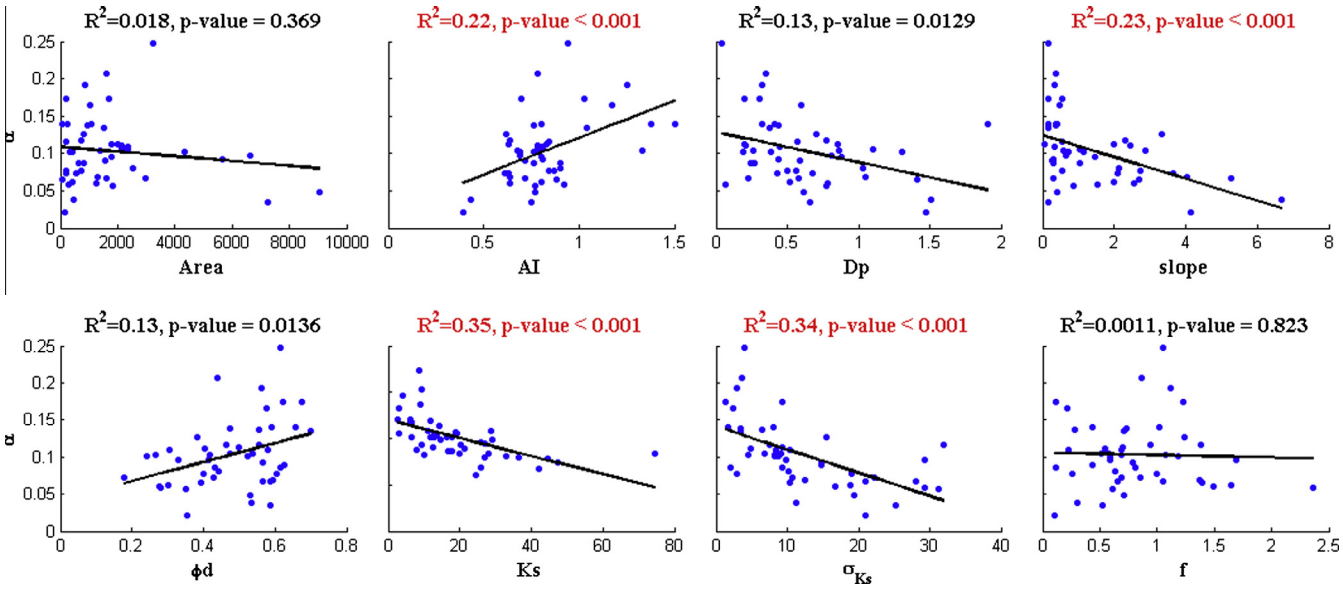

Fig. 5. Individual scatter plots of each predictor versus α.

(D_d), soil water storage capacity (ϕd), mean and standard deviation of surface saturated hydraulic conductivity (K_s, σ_{Ks}) and the vertical exponential rate of decay saturated hydraulic conductivity (f). Although these candidate variables individually do not explain much of the variances in α, β (i.e., $R^2 < 0.5$), many of them do have significant relationships with α and β (i.e., p-value < 1%). As seen from Figs. 5 and 6, the aridity index and topographic slope are closely related to both α and β, while α is also related to drainage density and the mean and standard deviation of surface saturated hydraulic conductivity.

In the next step, we determined variables that *together* give a better prediction of α and β. As R^2 always benefits from having more predictors, to avoid over-fitting, a variable selection procedure was carried out to identify the most influential predictors. Fig. 7 presents the frequency that each variable was selected by the three statistical criteria discussed earlier in Section 2.2.2 for α and β. For α, the variables selected more than half of the time for all three criteria are: drainage density (D_d), topographic slope (θ), mean saturated hydraulic conductivity at surface (K_s), soil water storage capacity (ϕd) and the decay parameter (f). For β, a smaller number of predictor variables were retained most often in all three methods (AIC, BIC and Lasso), and only aridity index (AI) and decay parameter (f) were selected. The resulting regressions are:

$$\alpha = \frac{0.21(\phi d)^{0.37} f^{0.17}}{D_d^{0.12}\exp(0.03\theta + 0.02K_s)} \tag{14a}$$

$$\beta = 2.27e^{-0.53AI} f^{0.05} \tag{14b}$$

As we can see from both equations, the decay parameter is found to be important for both α and β; α is also related to other soil and topographic properties while, interestingly, β is also influenced by climatic aridity index besides the decay parameter.

Table 2 presents the averaged R^2 values over the 50 runs, for the calibration and validation sets for the full models that kept all the candidate variables, and the reduced model with only the selected variables. A cross validation procedure is applied to reduce the bias due to our relatively small sample size. The model fits the data well for the training set both for the full model and the reduced new model with R^2 values larger than 0.8. Although R^2 drops in the testing dataset used for validation, the reduced model is more accurate than the over-fitted full model with R^2 improved from 0.32 to 0.54. The regression obtained for β is also good in the training dataset, with R^2 equal to or larger than 0.75. Although the prediction precision drops in the testing dataset, the reduced model improved R^2 by 80%. One possible reason for R^2 dropping from calibration to validation is the limited sample size, since only 12 catchments were used for validation: the small sample size may add variance to the prediction and decrease R^2 of the validation.

Fig. 8 is an example comparison plot of one flow event in a well-measured catchment in New York. Red dashed line is the recession calculated from the α and β derived from the recession analysis of the local catchment, the green line is the recession curve predicted by the fitted α and β estimated from Eqs. (14a) and (14b), while the black recession line is estimated using the average α and β values of all the study catchments. As we can see from the figure, while the flow predicted from the simple mean α and β is much larger than the measured recession curve, the recessions generated using the parameter estimates from Eqs. (14a) and (14b) match the observations much better, suggesting that the empirical regionalization approach presented here could provide decent predictions of flow recessions in these study catchments.

4. Discussion: interpretation of the derived functional forms of α, β

The derived functional forms for α and β (Eqs. (14a) and (14b)), though completely empirical, are still consistent with trends suggested by the application of hydraulic theory governing shallow subsurface flow on hillslopes expressed in the form of the Boussinesq equation (Brutsaert and Nieber, 1977; Rupp and Selker, 2005, 2006a,b). Since our work was carried out at catchment scale, and most of the previous analytical derivations were derived for a single aquifer at the hillslope scale, we would not expect similar functional forms for the storage–discharge relationship. However, the variables that are found to be important from our empirical analyses are the same as the variables that appear in these analytical results. For example, in the case of hydraulic theory, the coefficient of the recession–slope curves, α, for a homogeneous aquifer, was found to be a function of the hydraulic conductivity (K), average aquifer thickness (d), length of the river network (L), drainage area (A), and porosity (ϕ) (Brutsaert and Lopez, 1998,1999):

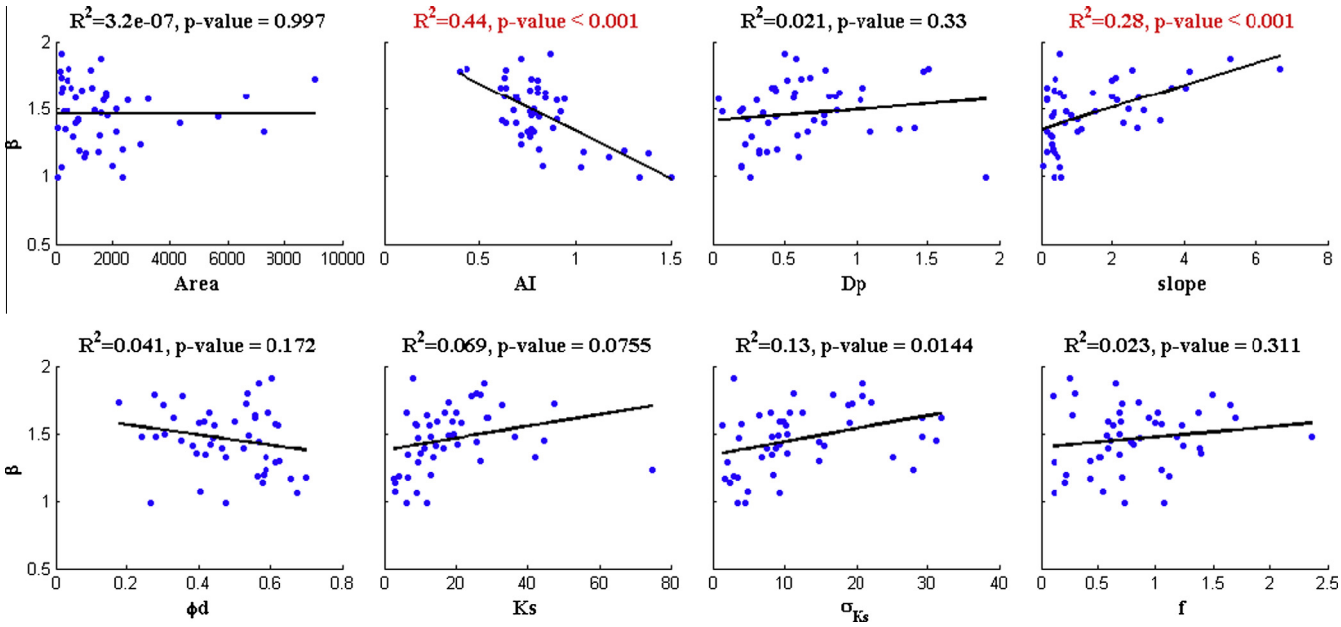

Fig. 6. Individual scatter plots of each predictor versus β.

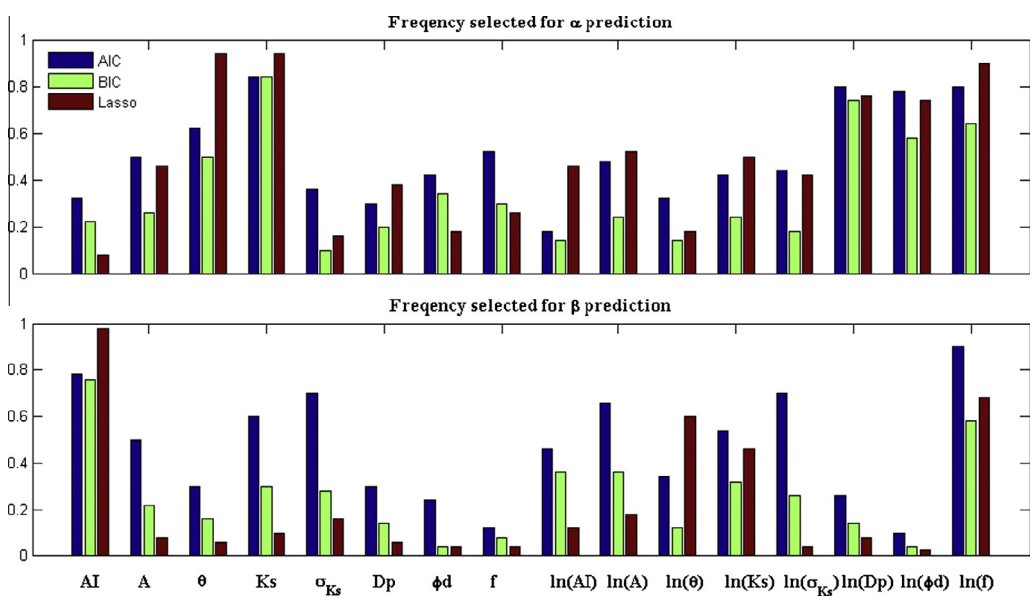

Fig. 7. Frequency selected for α and β prediction.

Table 2
The averaged R^2 of the full model with all the variables, and the new model with only the chosen variables after the selection.

		R^2_full model	R^2_new model
α	Calibration	0.84	0.73
	Validation	0.32	0.54
β	Calibration	0.84	0.75
	Validation	0.27	0.49

$$\alpha = \frac{\psi(\beta)(4Kd^2L^2/A)^{2-\beta}}{(\phi d)A} \tag{15}$$

where $\psi(\beta)$ is a polynomial function of β. In subsequent work (Rupp and Selker, 2005) showed that β can be strongly affected by the vertical decrease of the saturated hydraulic conductivity, and showed that $\beta = (2h+1)/(h+1)$, where h is a parameter of the power-law relationship of the saturated hydraulic conductivity (K) with depth. This is also the case in the results of our analysis here (i.e., Eqs. (14a) and (14b)), except that the stream length and drainage area were combined into a drainage density, as was done by Biswal and Marani (2010).

The analytical derivations of Rupp and Selker (2005) through the application of the Boussinesq equation to sloping aquifers highlighted the role of topographic slope, which is also confirmed in the present study. Finally, the study by Rupp and Selker (2005) also highlighted the impact of the vertical decrease of saturated hydraulic conductivity on the exponent β, although in their case they assumed a power law decay in the vertical (as opposed to the exponential decay used here). Rupp and Selker (2005) also

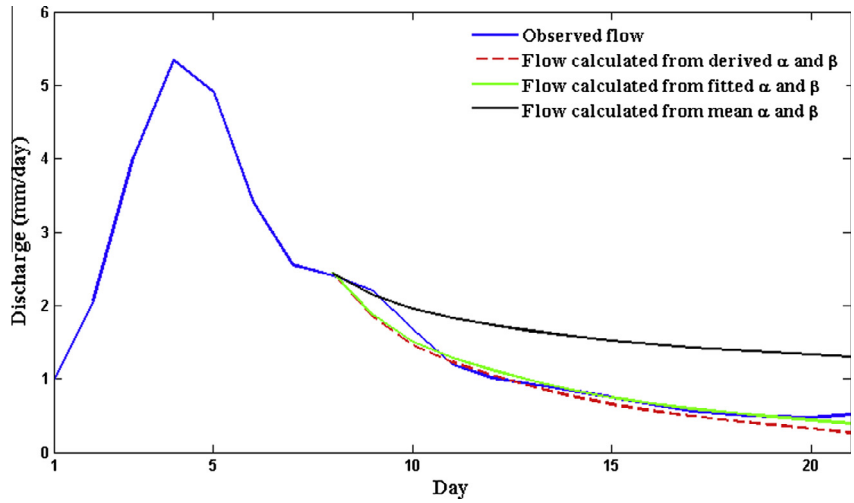

Fig. 8. Streamflow time series comparison in a well-measured catchment: blue line is the observed daily flow, red dashed line is the recession calculated from the α and β estimated from regression analysis, green line is the recession calculated from regional estimates of α and β obtained from Eqs. (14a) and (14b), black line is the recession calculated from the averaged α and β of the study catchments. (For interpretation of the references to colour in this figure legend, the reader is referred to the web version of this article.)

showed that it is the decrease in saturated hydraulic conductivity in the vertical that gives rise to the exponent β being greater than 2.

Our empirical analyses also show that the exponential decay rate of the saturated hydraulic conductivity is one of the two most influential variables governing the magnitude of the exponent β. In fact, the exponential decay parameter f is the only variable that is considered important for both the coefficient, α, and exponent, β. Although the importance of vertical decrease of hydraulic conductivity has been recognized and understood within the broader context of flow convergence (Chapman, 1999; Harman and Sivapalan, 2009), our study has helped to confirm it in many actual catchments. Although the estimate of the f parameter used here is only approximate due to paucity of measurements, its appearance in the regressions still underlines its importance in controlling the shape of the recession curve. Given the importance of this vertical decay parameter of the saturated hydraulic conductivity, further studies are needed to explore the impact of soil data quality on the estimates of the decay parameter and also the influence of different estimation methods.

Besides the vertical convergence of water movement controlled in this case by the vertical decay of the hydraulic conductivity, our results also indicate that the recession exponent at the catchment scale is also strongly related to the aridity index (*AI*). This climate impact is not explicitly included or needed in either the hydraulic theory or heterogeneity theory (Harman et al., 2009; Harman and Sivapalan, 2009). Not only was this parameter clearly selected in the reduced models, but the magnitude of the coefficient before it in the functional form for β is at least one order of magnitude larger than that of the hydraulic conductivity decay parameter. This inconsistency with hydraulic or heterogeneity theory is also apparent in the comparison of the expressions for α and β derived here with the equivalent results (not presented here for reasons of brevity) obtained by numerical simulation and up-scaling derived by Ali et al. (2014), in which case only the hydraulic conductivity, its variability in space (both vertical and lateral), and topographic slope were the most important parameters needed for regionalizing the recession curve parameters.

The fact that climate in the form of the aridity index, *AI*, has an impact on the shape and magnitude of the recession curves and the parameters α and β may be attributed to the possibility that variables such as K_s, ϕd, θ, and D_d may be individually and/or collectively modified by climate. This includes their spatial heterogeneity, including any co-variation with topography. A likely hypothesis for the occurrence of these effects is possible adaptation of topography and soils to the climate, mediated by vegetation, through the erosional and pedogenic processes that contribute to soil formations. Our empirical results show that β is more strongly related to *AI* but not α. This may be due to the influence of climate on the vegetation which, through the action of roots in soil development, thus leading to vertical gradients of soil hydraulic properties, such as the hydraulic conductivity, that are known to impact to the magnitude of β (Rupp and Selker, 2005).

Although co-dependence of soil properties on climate is yet to be taken into consideration by extant hydraulic and/or heterogeneity theories, the significant correlation between climate and the

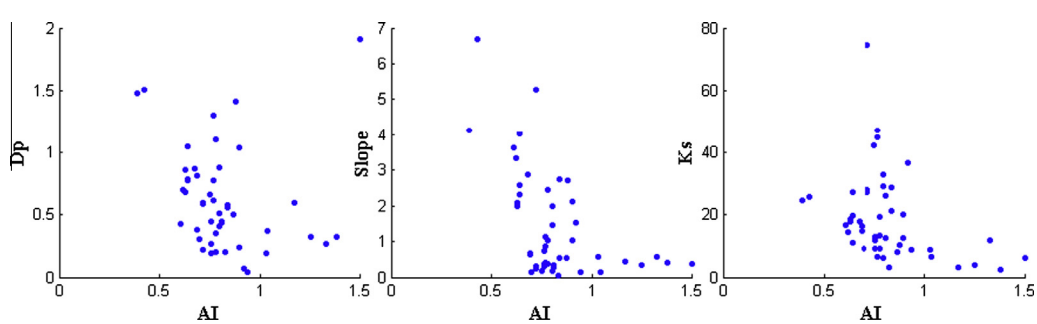

Fig. 9. Individual scatter plots of each predictor versus *AI*.

organized heterogeneity exhibited by many landscape properties has been highlighted in other research findings from the data analysis. For example, Wang and Wu (2013) found in 185 MOPEX catchments across the continental US that the scaled perennial drainage density decreases monotonically with *AI*. Likewise, Xu et al. (2012) found that in several Australian catchments the fractions of vegetation cover that are deep rooted perennial or shallow rooted ephemeral show a systematic relationship with *AI*. In the case of the 50 study catchments used here, we therefore explored possible co-dependence between climate and landscape properties, using the available data. Fig. 9 presents scatter plots of the relationships between topographic slope, drainage density, and saturated surface hydraulic conductivity. Given the use of eastern catchments that are relatively humid and vegetated, these preliminary results are not sufficient enough to claim that there is a strong dependence on climate, we do see a clear correlation between *AI* and the three landscape properties in these scatter plots, which is also consistent with the findings in the literature cited above. Nevertheless, given the correlations found in the recent empirical analyses and the statistically significant co-dependence of the β parameter on *AI*, these findings are worthy of more detailed analysis on a larger set of catchments (around the nation and around the world covering a larger range of climates and landscapes) that have the necessary soils and topographic data available. Moreover, further studies are also needed to explore the seasonal variation of α and β across the year with explicit inclusion of the role of ET on the recession parameters. These are beyond the scope of this study.

5. Conclusions

The goal of this study has been to develop an empirically-based parameterization of storage–discharge relations for subsurface stormflow for use in land surface models (LSMs) or catchment-scale rainfall–runoff models. The approach adopted capitalizes on a straightforward relationship between the storage–discharge relations and a catchment's recession curve (or the recession–slope relationship), followed by performing multiple regressions of the recession curve parameters against measurable climate, soil and topographic properties. This analysis also helped to identify the climatic and catchment characteristics that control the recession behavior without recourse to extant theory relating to shallow subsurface flow in heterogeneous catchments.

The analyses reported here were carried on 50 selected catchments mostly in the eastern half of the US. The parameters relating to a power-law type recession-slope curve, a coefficient α and the exponent β, were extracted from observed streamflow hydrographs in all 50 catchments during the winter period in order to minimize the influence of evapotranspiration. Three different model selection methods were applied to choose variables that would collectively help predict the empirically observed α and β values. This analysis showed that the soil water storage capacity, drainage density, topographic slope, mean saturated hydraulic conductivity at the surface and its vertical decay parameter with depth are essential for predicting α, while the aridity index and the parameter describing vertical decay of saturated hydraulic conductivity are the only variables needed for predicting β. This analysis resulted in statistically significant predictive relationships in terms of the predictor variables for both α and β.

The trends indicated by these empirically derived functional relationships are found to be consistent with corresponding expressions presented in the literature that were derived from extant hydraulic or heterogeneity theory. In this sense, these results are a confirmation of the predictions from existing theories. Yet, the empirical analyses also, for the first time, revealed the important role of climate, in the form of the aridity index, on the recession curve parameters. There is no explanation for this in existing theories, as also confirmed by the parallel work of Ali et al. (2014), which do not and cannot presently incorporate the effect of climate. We attributed this climate dependence to the adaptation of landscape properties (e.g., soil, vegetation and topography) to climate at the catchment scale. On the other hand, soil, vegetation and topography can also exert controls on the climate but at a scale much larger than the catchment scale, i.e., regional or global scale, by way of regulating moisture, energy and carbon cycling. Such co-independence of climate, soil, vegetation and topography across catchment, regional and global scales, as it occurred continuously over long timescales (e.g., geological time) without strong disturbance, can be called as co-evolution. We argue that this co-evolution hypothesis may provide a theoretical foundation for regionalization studies, which have been previously carried out in an empirical way. The investigation of the mechanisms underpinning this co-evolution hypothesis is nevertheless far beyond this study, and thus left for future study.

There remains the question of how to benefit from the regionalized equations derived in this paper for the original goal of the research: develop parameterizations of subsurface stormflow for land surface models. The statistical model derived here has in effect captured the net effects of co-evolution and is therefore useful for extrapolations in the region within which it was derived. Although the statistical model provides important insights into the factors that control the recession curves, due to the limited number of catchments and the relative humid climate of these catchments, its validity for extrapolation to regions other than the relatively humid eastern US is not clear. The empirical relationship may or may not change when one moves from the relatively humid catchments to more arid ones, since the physical meaning behind the statistical model is still not clear. But this empirical relationship could still serve as a reasonable initial guess for the parameterization in less humid regions. Furthermore, incorporation of this empirical relationship in land surface or catchment hydrology models could help verify and improve our findings and further understanding of the storage discharge relationship.

Further studies are needed to validate our results in the types of catchments that were excluded here, such as the ones in arid climates, or are dominated by confounding factors such as snowmelt or land use changes. On the other hand, parameterizations derived on the basis of traditional hydraulic theory (e.g., Ali et al., 2014) also have limitations, because so far they do not include the effects of co-evolution. There is therefore a clear need for a reconciliation of these approaches so that we can derive parameterizations that are based on widely applicable physics, and yet capture the net effects of co-evolution of climate, soils, topography and vegetation. Moreover, averages were used in this analysis as representative of the whole catchment, but this does not necessarily mean every hillslope contributes to the recession equivalently. It is likely that an active zone near the river network including local aquifers and banks, lakes and ponds, wetlands, etc. may play a more important role in the recession behavior. The relative contribution of these landscape elements to the recession curve requires further, more detailed study, and is left for further research.

Acknowledgements

This study was supported by the Office of Science of the U.S. Department of Energy as part of the IMPACTS project funded by the Earth System Modeling program to improve hydrologic parameterizations in land surface models for predicting changes in droughts in the future climate. PNNL is operated for DOE by Battelle Memorial Institute under Contract DE-AC05-76RLO1830.

References

Akaike, H., 1974. A new look at the statistical model identification. IEEE Trans. Autom. Control 19 (6), 716–723. http://dx.doi.org/10.1109/TAC.1974.1100705, MR 0423716.

Ali, M., Ye, S., Li, H.-Y., Huang, M.-Y., Leung, L.R., Fiori, A., Sivapalan, M., 2014. Regionalization of subsurface stormflow parameters for hydrologic models: up-scaling from physically based numerical simulations at hillslope scale. J. Hydrol., in press. http://dx.doi.org/10.1016/j.jhydrol.2014.07.018.

Anderson, R.M., Koren, V.I., Reed, S.M., 2006. Using SSURGO data to improve sacramento model a priori parameter estimates. J. Hydrol. 320 (1), 103–116.

Beven, K.J., 1997. TOPMODEL: a critique. Hydrol. Process. 11, 1069–1085.

Beven, K.J., Kirkby, M.J., 1979. Towards a simple, physically based, variable contributing area model of catchment hydrology. Hydrol. Sci. Bull. 24, 43–69.

Beven, K.J., Kirkby, M.J., Schofield, N., Tagg, A.F., 1984. Testing a physically based flood forecasting model (topmodel) for three U.K. catchments. J. Hydrol. 69 (1–4), 119–143. http://dx.doi.org/10.1016/0022-1694(84) 90159-8.

Biswal, B., Marani, M., 2010. Geomorphological origin of recession curves. Geophys. Res. Lett. 37, L24403. http://dx.doi.org/10.1029/2010GL045415.

Bliss, N.B., Waltman, S.W., Neale, A.C., 2010. Detailed soil information for hydrologic modeling in the conterminous United States. In: Amer. Geophys. Union, Fall Meeting, San Francisco, 13–17 December, 2010, EOS Transactions, Suppl., vol. 91: Abstract H43B-1227. Available online at: <http://www.agu.org/meetings/fm10/waisfm10adv.html>.

Brutsaert, W., Lopez, J.P., 1998. Basin-scale geohydrologic drought flow features of riparian aquifers in the southern Great Plains. Water Resour. Res. 34 (2), 233–240.

Brutsaert, W., Lopez, J.P., 1999. Comment on "basin-scale geohydrologic drought flow features of riparian aquifers in the southern Great Plains" – reply. Water Resour. Res. 35 (3), 911–911.

Brutsaert, W., Nieber, J.L., 1977. Regionalized drought flow hydrographs from a mature glaciated plateau. Water Resour. Res. 13 (3), 637–644.

Chapman, T.G., 1999. A comparison of algorithms for stream flow recession and baseflow separation. Hydrol. Process. 13 (5), 701–714.

Earls, J., Dixon, B., 2005. A comparative study of the effects of input resolution on the SWAT model. Ecol. Environ. 12, 213–222.

Eltahir, E.A.B., Yeh, P.J.F., 1999. On the asymmetric response of aquifer water level to floods and droughts in Illinois. Water Resour. Res. 35, 1199–1217.

Engelhardt, I., De Aguinaga, J.G., Mikat, H., Schuth, C., Lenz, O., Liedl, R., 2012. Complexity versus simplicity: an example of groundwater model ranking with the Akaike Information Criterion. Hydrol. Earth Syst. Sci. Discuss. 9, 9687–9714. http://dx.doi.org/10.5194/hessd-9-9687-2012.

Francini, M., Pacciani, M., 1991. Comparative analysis of several conceptual rainfall–runoff models. J. Hydrol. 122, 161–219.

Harman, C.J., Sivapalan, M., 2009. A similarity framework to assess controls on shallow subsurface flow dynamics in hillslopes. Water Resour. Res. 45, W01417. http://dx.doi.org/10.1029/2008WR007067.

Harman, C.J., Sivapalan, M., Kumar, P., 2009. Power law catchment-scale recessions arising from heterogeneous linear small-scale dynamics. Water Resour. Res. 45, W09404. http://dx.doi.org/10.1029/2008WR007392.

Hastie, T., Tibshirani, R., Friedman, J., 2009. The Elements of Statistical Learning: Data Mining, Inference and Prediction. Springer.

Hatfield, J.L., McMullen, L.D., Jones, C.S., 2009. Nitrate–nitrogen patterns in the Raccoon River Basin related to agricultural practices. J. Soil Water Conserv. 64, 190–199. http://dx.doi.org/10.2489/jswc.64.3.190.

Hou, Z., Huang, M., Leung, L.R., Lin, G., Ricciuto, D.M., 2012. Sensitivity of surface flux simulations to hydrologic parameters based on an uncertainty quantification framework applied to the Community Land Model. J. Geophys. Res. 117, D15108. http://dx.doi.org/10.1029/2012JD017521.

Huang, M., Liang, X., 2006. An assessment of impact of reducing parameters and identification of parameter uncertainties in the VIC-3L model with applications to ungauged basins. J. Hydrol. 320, 37–61.

Huang, M., Liang, X., Leung, L.R., 2008. A generalized subsurface flow parameterization considering subgrid spatial variability of recharge and topography. J. Hydrometeorol. 9 (6), 1151–1171.

Huang, M., Hou, Z., Leung, L.R., Ke, Y., Liu, Y., Fang, Z., Sun, Y., 2013. Uncertainty analysis of runoff simulations and parameter identifiability in the Community Land Model – evidence from MOPEX basins. J. Hydrometeorol., http://dx.doi.org/10.1175/JHM-D-12-0138.1.

Koster, R., Dirmeyer, P., Guo, Z., Bonan, G., Chan, E., Cox, P., Gordon, C.T., Kanae, S., Kowalczyk, E., Lawrence, D., Liu, P., Lu, C., Malyshev, S., McAvaney, B., Mitchell, K., Mocko, D., Oki, T., Oleson, K., Pitman, A., Sud, Y.C., Taylor, C.M., Verseghy, D., Vasic, R., Xue, Y., Yamda, T., 2004. Regions of strong coupling between soil moisture and precipitation. Science 305, 1138–1140.

Lawrence, D.M., Oleson, K.W., Flanner, M.G., Thornton, P.E., Swenson, S.C., Lawrence, P.J., Zeng, X., Yang, Z.L., Levis, S., Sakaguchi, K., Bonan, G.B., Slater, A.G., 2011. Parameterization improvements and functional and structural advances in version 4 of the Community Land Model. J. Adv. Model. Earth Syst. 3 (M03001), 2011M. http://dx.doi.org/10.1029/S000045.

Li, H., Sivapalan, M., Liu, D., Tian, F., 2010. Water and nutrient balances in a large tile-drained agricultural catchment: a distributed modeling study. Hydrol. Earth Syst. Sci. 14, 2259–2275. http://dx.doi.org/10.5194/hess-14-2259-2010.

Li, H., Huang, M., Wigmosta, M.S., Ke, Y., Coleman, A.M., Leung, L.R., Wang, A., Ricciuto, D.M., 2011. Evaluating runoff simulations from the Community Land Model 4.0 using observations from flux towers and a mountainous watershed. J. Geophys. Res. 116, D24120. http://dx.doi.org/10.1029/2011JD016276.

Liang, X., Lettenmaier, D.P., Wood, E.F., Burges, S.J., 1994. A simple hydrologically based model of land surface water and energy fluxes for general circulation models. J. Geophys. Res. 99 (14), 415–428.

Liang, X., Xie, Z.H., Huang, M.Y., 2003. A new parameterization for surface and groundwater interactions and its impact on water budgets with the variable infiltration capacity (VIC) land surface model. J. Geophys. Res. 108 (D16), 8613. http://dx.doi.org/10.1029/2002JD003090.

Lyon, S.W., Troch, P.A., 2010. Development and application of a catchment similarity index for subsurface flow. Water Resour. Res. 46, W03511. http://dx.doi.org/10.1029/2009WR008500.

Niu, G.-Y., Yang, Z.-L., Dickinson, R.E., Gulden, L.E., 2005. A simple TOPMODEL-based runoff parameterization (SIMTOP) for use in global climate models. J. Geophys. Res. 110 (D21), D21106.

Niu, G.-Y., Yang, Z.-L., Dickinson, R.E., Gulden, L.E., Su, H., 2007. Development of a simple groundwater model for use in climate models and evaluation with gravity recovery and climate experiment data. J. Geophys. Res. 112 (D7), D07103.

Oleson, K.W., Lawrence, D.M., Bonan, G.B., Flanner, M.G., Kluzek, E., Lawrence, P.J., Levis, S., et al., 2010. Technical description of version 4.0 of the Community Land Model (CLM). In: NCAR Technical Note NCAR/TN-478+STR, p. 257.

Oleson, K.E., Lawrence, D.M., Bonan, G., Drewniak, B., Huang, M., Koven, C.D., Levis, S., Li, F., Riley, W.J., Subin, Z.M., Swenson, S.C., Thornton, P.E., Bozbiyik, A., Fisher, R., Kluzek, E., Lamarque, J.-F., Lawrence, P.J., Leung, L.R., Muszala, S., Ricciuto, D.M., Sacks, W., Tang, J., Yang, Z.-L., 2013. Technical Description of version 4.5 of the Community Land Model (CLM), National Center for Atmospheric Research, Boulder, CO, June 2013. <http://www.cesm.ucar.edu/models/cesm1.2/clm/CLM45_Tech_Note.pdf>.

Ringeval, B., Decharme, B., Piao, S.L., Ciais, P., Papa, F., de Noblet-Ducoudré, N., Prigent, C., Friedlingstein, P., Gouttevin, I., Koven, C., Ducharne, A., 2012. Modelling sub-grid wetland in the ORCHIDEE global land surface model: evaluation against river discharges and remotely sensed data. Geosci. Model Dev. 5 (4), 941–962. http://dx.doi.org/10.5194/gmd-5-941-2012.

Robinson, J.S., Sivapalan, M., 1995. Catchment-scale runoff generation model by aggregation and similarity analyses. Hydrol. Process. 9 (5–6), 555–574.

Rupp, D., Selker, J., 2005. Drainage of a horizontal Boussinesq aquifer with a power law hydraulic conductivity profile. Water Resour. Res. 41, W11422. http://dx.doi.org/10.1029/2005WR004241.

Rupp, D.E., Selker, J.S., 2006a. Information, artifacts, and noise in dQ/dt – Q recession analysis. Adv. Water Resour. 29, 154–160.

Rupp, D.E., Selker, J.S., 2006b. On the use of the Boussinesq equation for interpreting recession hydrographs from sloping aquifers. Water Resour. Res. 42, W12421. http://dx.doi.org/10.1029/2006WR005080.

Schwarz, G.E., 1978. Estimating the dimension of a model. Ann. Stat. 6 (2), 461–464. http://dx.doi.org/10.1214/aos/1176344136.

Seneviratne, S.I., Corti, T., Davin, E.L., Hirschi, M., Jaeger, E.B., Lehner, I., Orlowsky, B., Teuling, A.J., 2010. Investigating soil moisture-climate interactions in a changing climate: a review. Earth Sci. Rev. 99 (3–4), 125–161.

Shaw, S.B., Riha, S.J., 2012. Examining individual recession events instead of a data cloud: using a modified interpretation of dQ/dt – Q streamflow recession in glaciated watersheds to better inform models of low flow. J. Hydrol. 434–435, 46–54.

Stoelzle, M., Stahl, K., Weiler, M., 2013. Are streamflow recession characteristics really characteristics? Hydrol. Earth Syst. Sci. 17, 817–828.

Szilagyi, J., Parlange, M.B., Albertson, J.D., 1998. Recession flow analysis for aquifer parameter determination. Water Resour. Res. 34 (7), 1851–1857.

Tague, C., Grant, G., 2004. A geological framework for interpreting the low-flow regimes of Cascade streams, Willamette River Basin, Oregon. Water Resour. Res. 40, W04303. http://dx.doi.org/10.1029/2003WR002629.

Todini, E., 1996. The ARNO rainfall–runoff model. J. Hydrol. 175, 339–382.

Troch, P.A., Carrillo, G.A., Heidbüchel, I., Rajagopal, S., Switanek, M., Volkmann, T.H.M., Yaeger, M., 2008. Dealing with landscape heterogeneity in watershed hydrology: a review of recent progress toward new hydrological theory. Geogr. Compass 2. http://dx.doi.org/10.1111/j.1749-8198.2008.00186.x.

Troch, P.A. et al., 2013. The importance of hydraulic groundwater theory in catchment hydrology: the legacy of Wilfried Brutsaert and Jean-Yves Parlange. Water Resour Res. 49, 5099–5116. http://dx.doi.org/10.1002/wrcr.20407.

Viney, N.R., Sivapalan, M., 2004. A framework for scaling of hydrologic conceptualizations based on a disaggregation–aggregation approach. Hydrol. Process. 18 (8), 1395–1408.

Vogel, R.M., Kroll, C.N., 1992. Regional geohydrologic–geomorphic relationships for the estimation of low-flow statistics. Water Resour. Res. 28 (9), 2451–2458.

Wang, D., Hejazi, M., 2011. Quantifying the relative contribution of the climate and direct human impacts on mean annual streamflow in the contiguous United States. Water Resour. Res. 47, W00J12. http://dx.doi.org/10.1029/2010WR010283.

Wang, D., Wu, L., 2013. Similarity between runoff coefficient and perennial stream density in the Budyko framework. Hydrol. Earth Syst. Sci. 17, 315–324. http://dx.doi.org/10.5194/hess-17-315-2013.

Warrach, K., Stieglitz, M., Mengelkamp, H.T., Raschke, E., 2002. Advantages of a topographically controlled runoff simulation in a soil-vegetation-atmosphere transfer model. J. Hydrometeorol. 3 (4), 131–148.

Wittenberg, H., Sivapalan, M., 1999. Watershed groundwater balance estimation using streamflow recession analysis and baseflow separation. J. Hydrol. 219, 20–33.

Xu, X., Yang, D., Sivapalan, M., 2012. Assessing the impact of climate variability on catchment water balance and vegetation cover. Hydrol. Earth Syst. Sci. 16, 43–58.

Ye, S., Yaeger, M., Coopersmith, E., Chang, L., Sivapalan, M., 2012. Exploring the physical controls of regional patterns of flow duration curves, Part 2: role of seasonality, the regime curve, and associated process controls. Hydrol. Earth Syst. Sci. http://dx.doi.org/10.5194/hess-16-1-2012.